

Approaching the double-Heisenberg-scaling sensitivity in the Tavis-Cummings model

Yuguo Su,¹ Hai-Long Shi,^{2,3,*} Xiao-Guang Wang,⁴ Chaohong Lee,⁵ and Xi-Wen Guan^{1,3,6,7,†}

¹*Innovation Academy for Precision Measurement Science and Technology,
Chinese Academy of Sciences, Wuhan 430071, China*

²*QSTAR and INO-CNR, Largo Enrico Fermi 2, 50125 Firenze, Italy*

³*Hefei National Laboratory, Hefei 230088 China*

⁴*Key Laboratory of Optical Field Manipulation of Zhejiang Province and Department of Physics,
Zhejiang Sci-Tech University, Hangzhou 310018, China*

⁵*College of Physics and Optoelectronic Engineering, Shenzhen University, Shenzhen 518060, China*

⁶*NSFC-SPTP Peng Huanwu Center for Fundamental Theory, Xi'an 710127, China*

⁷*Department of Fundamental and Theoretical Physics, Research School of Physics,
Australian National University, Canberra ACT 0200, Australia*

The pursuit of quantum-enhanced parameter estimations without the need for nonclassical initial states has long been driven by the goal of achieving experimentally accessible quantum metrology. In this paper, employing a coherent averaging mechanism, we prove that the prototypical cavity-quantum electrodynamics (QED) system, such as the Tavis-Cummings (TC) model, enables us to achieve not only the Heisenberg scaling (HS) precision in terms of the average photon number but also the double-HS sensitivity concerning both the average photon and atom numbers. Such a double sensibility can be experimentally realized by introducing either photon- or atom-number fluctuations through quantum squeezing. Furthermore, we discuss the methodology to achieve this double-HS precision in a realistic experimental circumstance where the squeezing is not perfect. Our results provide insights into understanding the coherent averaging mechanism for evaluating quantum-enhanced precision measurements and also present a usable metrological application of the cavity QED systems.

I. INTRODUCTION

Quantum metrology endeavors to achieve high-precision measurements of physical parameters by exploiting metrological resources, including quantum entanglement [1–8] and quantum squeezing [9–17], etc. Remarkable progress in experimental technology has facilitated extensive applications of quantum metrology in a variety of fields such as atomic clocks [18–20], gravitational wave detectors [21], magnetometry [22–27] and quantum imaging [28–32]. A central challenge of quantum metrology involves identifying inherent metrological limitations and designing accessible schemes to enhance the precision of parameter estimation. For this purpose, it is necessary to analyze the scaling behavior of the quantum Fisher information (QFI), which poses the theoretical limit for estimating an unknown parameter γ via the quantum Cramér-Rao bound [33] $\delta\gamma \geq 1/\sqrt{\nu\mathcal{F}_\gamma}$. This bound can be asymptotically approached by increasing the number of independent measurements ν .

In the scenario of the quantum phase estimation, the highest achievable precision using the separable N -particle states is known as the standard quantum limit (SQL), represented by $\mathcal{F}_\gamma \propto N$. However, the entangled states are indispensable for surpassing this limit to approach the Heisenberg limit (HL), i.e., $\mathcal{F}_\gamma \propto N^2$. Instead of directly employing entangled probes, numerous alternative approaches have been explored to enhance

measurement precisions by harnessing the quantum features arising from many-body physics [34, 35], such as criticality-enhanced metrology [25, 36–42], chaotic quantum metrology [43–45], quantum Zeno effect-based metrology [46], or by optimal adaptive quantum controls [47–49].

A promising scheme called “coherent averaging” [50–52] has been proposed, where a central spin (a “quantum bus”) is coupled with a cavity. Thus, it becomes possible to utilize an initial product state to attain the Heisenberg scaling (HS) sensitivity for estimating a global phase. Consequently, a crucial question naturally arises: Can we improve measurement precision by enlarging the quantum bus from a single atom to N atoms? Moreover, is it feasible to extend the coherent averaging mechanism for precise estimation of a non-global parameter?

In this paper, we report on a realization of the double-HS sensitivity $\mathcal{F}_\gamma \propto N^2\bar{n}^2$ with respect to the number of two-level atoms N and the average number of photons \bar{n} in the Tavis-Cummings (TC) model [53], see Fig. 1. This model provides a versatile platform for investigating the interplay between light and matter in the paradigm of quantum optics and quantum metrology. In contrast to the previous scenario with a single central spin, the N atoms in the TC model, acting as a quantum bus, could show the collective interplay with the light and involve quantum resources. We claim that the coherent averaging mechanism naturally emerges, enabling the estimation of even a non-global parameter, such as a weak magnetic field, in the TC model. Furthermore, we demonstrate that the introduction of quantum fluctuations in photon or atom numbers, achieved through

* hailong.shi@ino.cnr.it

† xiwen.guan@anu.edu.au

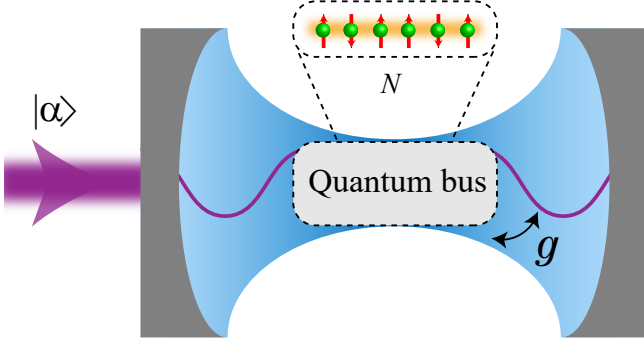


Figure 1. Cavity-QED setup. A coherent field $|\alpha\rangle$ with \bar{n} photons is injected into the cavity and couples to N trapped two-level atoms (green) with the coupling strength g . The N atoms, serving as a quantum bus, exhibit equal coupling strengths to the optical field, forming the TC model. We will estimate a non-global parameter, the strength of a weak magnetic field h , appearing in the Hamiltonian (1).

squeezing, allows for the attainment of double-HS sensitivity. Our findings highlight a potential application of the TC model to the experimental implementation of the high-precision quantum measurement with experimentally accessible quantum resources.

In Sec. II, we present the TC model, and employ the time-averaged method to derive an effective description of the TC model. In Sec. III, we introduce the metrological scheme and derive the analytic QFI to quantify measurement precision. The impact of selecting different initial states on QFI is comprehensively discussed in Sec. IV. Finally, Sec. V summarizes and discusses our findings.

II. TAVIS-CUMMINGS MODEL AND ITS EFFECTIVE DESCRIPTION

The TC model characterizes the coupling of a single bosonic cavity mode to a collection of N two-level atoms (or spin-1/2 spins), as illustrated in Fig. 1:

$$H = (h + \omega_0)J_z + \omega_a a^\dagger a + H_1, \quad (1)$$

$$H_1 = g(a^\dagger J_- + a J_+), \quad (2)$$

where H_1 denotes the interaction Hamiltonian and $J_{x,y,z} = \sum_{j=1}^N \sigma_j^{x,y,z}/2$, $J_\pm = J_x \pm iJ_y$ are the collective spin operators; a^\dagger and a are creation and annihilation operators for the cavity mode; ω_0 , ω_a and $2g$ are the original spin transition, the cavity frequency and the single-photon Rabi frequency; h is the magnetic field to be estimated. Throughout the paper, we set the Planck constant $\hbar = 1$. Next, we will derive an effective metrological Hamiltonian for estimating the weak magnetic field h and prove that the coherent averaging mechanism will emerge.

After applying the unitary transformation $U_1 = \exp[-i(\omega J_z + \omega_a a^\dagger a)t]$, the total Hamiltonian (1) in

the interaction picture takes the form:

$$H^{(I)} = i\frac{dU_1^\dagger}{dt}U_1 + U_1^\dagger H U_1 = g(a^\dagger J_- e^{-i\Delta t} + \text{H.c.}), \quad (3)$$

where $\Delta = \omega - \omega_a$ is the effective detuning and $\omega \equiv \omega_0 + h$. Utilizing the time-averaged method of the Ref. [54], the interaction Hamiltonian $H^{(I)} = \sum_{i=1}^N (f_i^\dagger e^{-i\Delta_i t} + \text{H.c.})$ could be rewritten as the following compact form

$$\begin{aligned} H^{(I)} &\approx \sum_{i,j=1}^N \frac{1}{\Delta_{ij}} [f_i^\dagger, f_j] e^{i(\Delta_i - \Delta_j)t} \\ &= -\frac{g^2}{\Delta} [a^\dagger J_-, a J_+] \\ &= \frac{g^2}{\Delta} (2J_z a^\dagger a + J_+ J_-), \end{aligned} \quad (4)$$

where the operator $f_i = g a \sigma_i^+ / 2$, the i -th effective detuning $\Delta_i \equiv \Delta$ and the harmonic average frequency $\Delta_{ij} \equiv |2\Delta_i \Delta_j / (\Delta_i + \Delta_j)| = |\Delta| > 0$ correspond to our system. The validity of the approximation in Eq. (4) is guaranteed by the fact that the high-frequency contribution can be neglected from the average [55], which relies on the large detuning condition, i.e., $\Delta \gg g\sqrt{N}$ and $\Delta \gg g\sqrt{N^2/\bar{n}}$. $\bar{n} \equiv \langle a^\dagger a \rangle$ denotes the average photon number. Returning to the Schrödinger picture, we obtain the effective Hamiltonian as follows

$$\begin{aligned} H_{\text{eff}}^{(s)} &= i\frac{dU_1}{dt}U_1^\dagger + U_1 H^{(I)} U_1^\dagger \\ &\simeq \omega J_z + \omega_a a^\dagger a + \frac{2g^2}{\Delta} J_z a^\dagger a + \frac{g^2}{\Delta} J_+ J_-, \end{aligned} \quad (5)$$

Generally, the average photon number is much larger than the number of up spins, i.e., $\bar{n} \gg \langle J_z \rangle = \langle [J_+, J_-] \rangle / 2$, then the Hamiltonian (5) can be further reduced as follows:

$$H_{\text{eff}} = \omega J_z + \omega_a a^\dagger a + \frac{2g^2}{\Delta} J_z a^\dagger a. \quad (6)$$

It should be emphasized that the estimated parameter h now appears in the coupling term, i.e., $\Delta = \omega_0 - \omega_a + h$, which reveals the existence of the coherent averaging mechanism in the TC model. The effective Hamiltonian (6) without dissipation can be achievable for the strong light-atom interaction of the cavity-atom system [56–59]. We will demonstrate that the Hamiltonian (6) enables achieving \bar{n}^2 HS sensitivity without requiring initial entanglement or squeezing between atoms and photons due to the emergent coherent averaging mechanism, i.e., the effective coupling term $J_z a^\dagger a$. We will also show an attainable double-Heisenberg-scaling sensibility in measuring the weak field h by introducing some quantum resources.

III. METROLOGICAL SCHEME AND QUANTUM FISHER INFORMATION

We consider an initial probe state of a bipartite product of an optical component and an atomic component,

i.e., $\rho = \rho_{\text{op}} \otimes \rho_{\text{at}}$. The optical component is chosen as a single-mode Gaussian state [60, 61]

$$\rho_{\text{op}} = D(\alpha) S(\xi) \rho_{\text{th}} S^\dagger(\xi) D^\dagger(\alpha), \quad (7)$$

which gives a displaced squeezed thermal state (DSTS). In the above equation, $\rho_{\text{th}} = \sum_n p_n |n\rangle\langle n|$ denotes a thermal state with a probability amplitude $p_n = n_{\text{th}}^n / (1 + n_{\text{th}})^{n+1}$, where n_{th} is the thermal photon number and $|n\rangle$ denotes the Fock state. While $D(\alpha) = \exp(\alpha a^\dagger - \alpha^* a)$ is the displacement operator with a displacement parameter $\alpha = |\alpha| \exp(i\zeta)$ ($|\alpha| \geq 0$) and $S(\xi) = \exp(-\xi a^{\dagger 2}/2 + \xi^* a^2/2)$ is a squeezing operator with a squeezing parameter $\xi = r \exp(i\vartheta)$ ($r \geq 0$). In general, the optical quantum state ρ_{op} can be characterized by the parameters $(|\alpha|, \zeta, r, \vartheta, n_{\text{th}})$, which represent the displacement amplitude, the displacement angle, the squeezing amplitude, the squeezing angle and the thermalization, respectively.

Following the unitary evolution $\rho(t) = U(t)\rho U^\dagger(t)$ where $U(t) = e^{-iH_{\text{eff}}t}$, the estimated parameter h will be encoded into the evolved state $\rho(t)$. The precision associated with estimating the magnetic field h is governed by the quantum Cramér-Rao bound [33]

$$\delta h \geq \frac{1}{\sqrt{\mathcal{F}_h}}, \quad (8)$$

where the QFI can be determined by the following formula [62, 63]

$$\mathcal{F}_h = \sum_{p_i \in \mathcal{S}} 4p_i \langle \Psi_i | \mathcal{H}_h^2 | \Psi_i \rangle - \sum_{p_i, p_j \in \mathcal{S}} \frac{8p_i p_j}{p_i + p_j} |\langle \Psi_i | \mathcal{H}_h | \Psi_j \rangle|^2. \quad (9)$$

Here, $|\Psi_i\rangle$ is i -th eigenstate of the initial system $\rho = \rho_{\text{op}} \otimes \rho_{\text{at}}$ with the eigenvalue p_i , $\mathcal{S} = \{p_i \in \{p_i\} | p_i \neq 0\}$ is the support of the initial density matrix. Based on the effective Hamiltonian (6), the generator of quantum sensing is given by

$$\mathcal{H}_h = i[\partial_h U^\dagger(t)]U(t) = \left(\frac{2g^2}{\Delta^2} a^\dagger a - 1 \right) t J_z. \quad (10)$$

We restrict the initial optical cavity to a Gaussian state (7) due to its encompassment of commonly encountered quantum states in experiments, such as the coherent and squeezed states. By substituting the initial system $\rho = \rho_{\text{op}} \otimes \rho_{\text{at}}$ (7) and the generator (10) of quantum sensing into the definition of the QFI (9), we obtain the QFI as follows

$$\begin{aligned} \mathcal{F}_h = 4t^2 \left\{ \left(1 - \frac{2g^2}{\Delta^2} \bar{n} \right)^2 \text{Var}(J_z) + \frac{4g^4}{\Delta^4} \text{Var}(a^\dagger a) \langle J_z^2 \rangle \right. \\ \left. - \frac{4g^4}{\Delta^4} n_{\text{th}} (n_{\text{th}} + 1) \langle J_z \rangle^2 \left[\frac{\cosh 4r (2n_{\text{th}} + 1)^2 + 1}{4n_{\text{th}} (n_{\text{th}} + 1) + 2} \right] \right. \\ \left. + \frac{4|\alpha|^2}{2n_{\text{th}} + 1} [1 + 2 \sinh^2 r - \sinh 2r \cos(2\zeta - \vartheta)] \right\}, \quad (11) \end{aligned}$$

where

$$\begin{aligned} \text{Var}(a^\dagger a) = \frac{\sinh^2 2r}{2} (2n_{\text{th}}^2 + 2n_{\text{th}} + 1) \\ + |\alpha|^2 (2n_{\text{th}} + 1) [\cosh 2r - \sinh 2r \cos(2\zeta - \vartheta)] \\ + (1 + 2 \sinh^2 r)^2 n_{\text{th}} (n_{\text{th}} + 1), \quad (12) \end{aligned}$$

is the photon-number fluctuation, $\langle \cdot \rangle$ represents the expectation with respect to the initial state, and $\text{Var}(O) = \langle O^2 \rangle - \langle O \rangle^2$ is the variance of the operator O . Subsequently, we will proceed to demonstrate that the analytical outcome (11) for the QFI offers highly practical theoretical insights for metrological applications within the cavity QED systems.

IV. RESULTS

A. Coherent spin state with different photon states

In this section, we fix the atom state to be uncorrelated, namely separable states, and explore the conditions that allow a photon state to achieve a double-HS precision. Separable spin-coherent states $\rho_{\text{at}} = |\mu\rangle_{\text{at}} \langle \mu|$ are given by [64]

$$|\mu\rangle = \frac{\exp(\mu J_-)}{(1 + |\mu|^2)^j} |0\rangle = \frac{1}{(1 + |\mu|^2)^j} \sum_{p=0}^{2j} \sqrt{\frac{(2j)!}{p!(2j-p)!}} \mu^p |p\rangle, \quad (13)$$

where $|p\rangle \equiv |j, j-p\rangle$ with $|j, j\rangle = |0\rangle$, being the eigenstate of J_z for $j = N/2$. Meanwhile, the phase parameter μ is parameterized by the angles (θ, ϕ) via the stereographic projection $\mu = e^{i\phi} \tan(\theta/2)$ [$\theta \in [0, \pi)$ and $\phi \in [0, 2\pi)$]. In order to ascertain the separability of $|\mu\rangle$, we can rewrite it as

$$|\mu\rangle \equiv |\theta, \phi\rangle = \bigotimes_{i=1}^N \left(\cos \frac{\theta}{2} |\uparrow\rangle_i + e^{i\phi} \sin \frac{\theta}{2} |\downarrow\rangle_i \right), \quad (14)$$

which is expressed as the tensor product of identical qubits, thereby leading us to categorize it as a classical atom state.

Optical coherent state.—Firstly, we consider the photon state as a classical coherent state (CS) $|\psi\rangle_{\text{op}} = |\alpha\rangle = D(\alpha)|0\rangle$, where $|\psi\rangle_{\text{op}}$ is the wavefunction of the reduced density matrix $\rho_{\text{op}} = |\psi\rangle_{\text{op}} \langle \psi|$. From Eqs. (11) and (13), we obtain

$$\begin{aligned} \mathcal{F}_h^{\text{CS}} = 4t^2 \left[\left(1 - \frac{2g^2}{\Delta^2} \bar{n} \right)^2 \text{Var}(J_z) + \frac{4g^4}{\Delta^4} \text{Var}(a^\dagger a) \langle J_z^2 \rangle \right] \\ = 4t^2 \left[\left(1 - \frac{2g^2}{\Delta^2} \bar{n} \right)^2 \frac{N}{4} \sin^2 \theta + \frac{g^4}{\Delta^4} \bar{n} N (\sin^2 \theta + N \cos^2 \theta) \right], \quad (15) \end{aligned}$$

where $n_{\text{th}} = 0$, $\bar{n} = |\alpha|^2$, $\text{Var}(J_z) = (N \sin^2 \theta) / 4$ and $\text{Var}(a^\dagger a) = \bar{n}$. Under the large average photon number condition ($\bar{n} \gg N$ and $2g^2\bar{n}/\Delta^2 \gg 1$), the above expression of QFI becomes

$$\mathcal{F}_h^{\text{CS}} \approx t^2 \frac{16g^4}{\Delta^4} \bar{n}^2 \text{Var}(J_z) = \frac{4g^4}{\Delta^4} t^2 N \bar{n}^2 \sin^2 \theta, \quad (16)$$

that suggests the maximum QFI $\mathcal{F}_h^{\text{CS}} \approx 4g^4 t^2 N \bar{n}^2 / \Delta^4$ for $\theta = \pi/2$. Hence, the result (16) gives the HS precision ($\propto \bar{n}^2$) through the utilization of the coherent averaging mechanism without using any entanglement of the initial state. In particular, the initial probe states are totally classical in the sense that the photon state is a coherent state and the atom state is a separable spin-coherent state.

The QFI provides the optimal measurement precision by optimizing over all positive operator-valued measurements. However, not all the experimental measurements can reach the precision limit bounded by the QFI, i.e., $\delta h \simeq 1/\sqrt{\mathcal{F}_h}$. The actual measurement precision δh is given by the error-propagation formula

$$\delta^2 h = \frac{\text{Var}[M(t)]}{|\partial_h \langle M(t) \rangle|^2}, \quad (17)$$

where M is an observable to be determined. In our case, we choose the $M = J_\varphi \equiv J_x \cos \varphi + J_y \sin \varphi$. By using the Baker-Campbell-Hausdorff formula [65] and the effective Hamiltonian (6), we find

$$\begin{aligned} M(t) &= e^{itH_{\text{eff}}} M e^{-itH_{\text{eff}}} \\ &= \frac{1}{2} \left[J_+ e^{-i(\varphi - \hat{\nu}t)} + J_- e^{i(\varphi - \hat{\nu}t)} \right], \\ M^2(t) &= \frac{1}{4} \left[N \left(\frac{N}{2} + 1 \right) - 2J_z^2 + J_+^2 e^{-2i(\varphi - \hat{\nu}t)} + J_-^2 e^{2i(\varphi - \hat{\nu}t)} \right], \end{aligned}$$

where $\hat{\nu} \equiv \omega_0 + h + 2g^2 a^\dagger a / \Delta$. For an initial spin-coherent state $|\theta, \phi\rangle$, Eq. (13), the expectation values are given by

$$\langle M(t) \rangle = \frac{N}{2} \sin \theta \cos(\nu t + \phi - \varphi), \quad (18)$$

$$\begin{aligned} \langle M^2(t) \rangle &= \frac{1}{16} N \{ N + 3 + (1 - N) \cos 2\theta \\ &\quad + 2(N - 1) \sin^2 \theta \cos[2(\nu t + \phi - \varphi)] \}, \quad (19) \end{aligned}$$

where $\nu \equiv \omega_0 + h + 2g^2\bar{n}/\Delta$. By substituting Eqs. (18) and (19) into the error-propagation formula (17), we have

$$(\delta h)^2 = \frac{\csc^2 \theta \csc^2(\nu t + \phi - \varphi) - \cot^2(\nu t + \phi - \varphi)}{N t^2 \left(\frac{2g^2}{\Delta^2} \bar{n} - 1 \right)^2} \quad (20)$$

$$\gtrsim \frac{\csc^2 \theta \csc^2(\nu t + \phi - \varphi) - \cot^2(\nu t + \phi - \varphi)}{4t^2 \frac{g^4}{\Delta^4} N \bar{n}^2}, \quad (21)$$

when the average photon number satisfies $2g^2\bar{n}/\Delta^2 \gg 1$. By choosing $\theta = \pi/2$, the greatest lower bound is taken as follows

$$(\delta h)^2 \gtrsim \frac{1}{4t^2 \frac{g^4}{\Delta^4} N \bar{n}^2}. \quad (22)$$

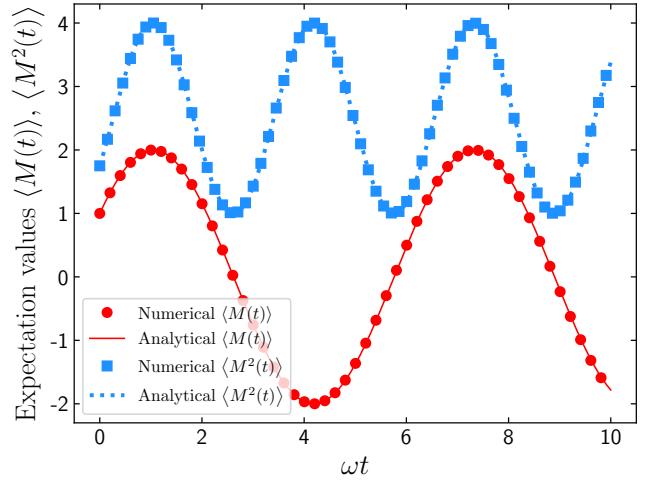


Figure 2. Expectation values $\langle M(t) \rangle$, $\langle M^2(t) \rangle$ for the initial state $|\psi\rangle = |\alpha\rangle \otimes |\mu\rangle$ versus the rescaled time ωt , with the spin number $N = 4$, the average photon number $\bar{n} = 100$, the original atomic transition frequency $\omega_0/(2\pi) = 6.9$ GHz, the cavity frequency $\omega_a/(2\pi) = 6.89$ GHz, the Rabi frequency $g/(2\pi) = 1.05$ MHz, the magnetic field $h = 1$ mHz, the parameterized angles $\theta = \pi/2$ and $\phi = 0$, the rotation angle $\varphi = \pi/3$. The red circles and blue squares represent the numerical results obtained from the original Hamiltonian (1); meanwhile, the solid red curve and blue dotted curve denote the analytical results obtained from the effective Hamiltonian (6). The parameters used in the calculation are similar to the ones given in Ref. [56], and numerical computations are performed by QuTip [66].

The validity of effective Hamiltonian is checked in Fig. 2 by comparing the expectation values obtained from the original Hamiltonian (1) and from analytic results (19) based on the effective Hamiltonian (6). Figure 3 shows that the optimal measurement precision determined by the QFI (15), i.e., the HS precision, can be achieved by performing measurements on the spin part.

Optical squeezed vacuum state.—In the second case, we replace the classical coherent photon state with a squeezed vacuum state (SVS) $|\psi\rangle_{\text{op}} = |\xi\rangle \equiv S(\xi)|0\rangle$. By invoking Eq. (11) with $|\alpha|^2 = n_{\text{th}} = 0$, $\text{Var}(J_z) = 0$ and $\langle \mu | J_z^2 | \mu \rangle = N^2/4$ for $\theta = 0$, the associated QFI is given by

$$\mathcal{F}_h^{\text{SVS}} = t^2 \frac{16g^4}{\Delta^4} \text{Var}(a^\dagger a) \langle J_z^2 \rangle = t^2 \frac{2g^4}{\Delta^4} N^2 \sinh^2 2r. \quad (23)$$

Given that it is perfect squeezing $\bar{n} = \sinh^2 r$ in this scenario and considering substantial quantum fluctuation such that $\text{Var}(a^\dagger a) = 2 \sinh^2 r \cosh^2 r \geq 2\bar{n}^2$, we further approximate Eq. (23) as

$$\mathcal{F}_h^{\text{SVS}} \geq \frac{8g^4}{\Delta^4} t^2 N^2 \bar{n}^2, \quad (24)$$

which implies the attainment of the double-HS precision ($\propto N^2 \bar{n}^2$) through the utilization of an SVS as the only resource state. We observe that the double-HS precision elucidated by Eq. (23) is essentially attributed to

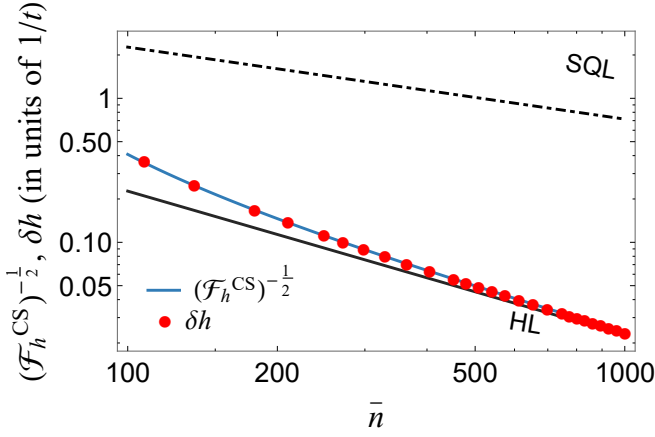


Figure 3. QFI $\mathcal{F}_h^{\text{CS}}$ and measurement precision δh (in units of $1/t$) of the cavity-QED system versus the average photon number \bar{n} , with the spin number $N = 4$, the original atomic transition frequency $\omega_0/(2\pi) = 6.9$ GHz, the cavity frequency $\omega_a/(2\pi) = 6.89$ GHz, the Rabi frequency $g/(2\pi) = 1.05$ MHz, the magnetic field $h = 1$ mHz, the rotation angle $\theta = \pi/2$. The blue line stands for the QFI $\mathcal{F}_h^{\text{CS}}$ obtained from Eq. (15); meanwhile, the red circles denote the measurement precision δh obtained from numerical calculation via the error-propagation-formula. The black dotted-dashed line is for SQL, and the black line denotes the HL. Our setting refers to the experimental parameters given in Ref. [56].

the fluctuation in photon number, exhibiting the scaling of \bar{n}^2 induced by the SVS. Consequently, the double-HS contribution exists in the QFI $\mathcal{F}_h^{\text{SVS}} \propto \text{Var}(a^\dagger a) \langle J_z^2 \rangle \propto \bar{n}^2 N^2$, regardless of whether the atom state is classical or nonclassical. This presents an avenue for achieving the double-HS precision, accomplished by harnessing the photon-number fluctuations engendered by squeezed photon states.

Displaced squeezed vacuum state.—In current realistic experimental capability, it is, however, hard to prepare a perfect squeezed photon state. It often involves the simultaneous coexistence of both squeezing and displacement. To elucidate the distinct roles played by the optical displacement and the optical squeezing, we consider the initial state is a product state $|\psi\rangle = |\alpha, \xi\rangle \otimes |\mu\rangle$, where the optical part is a displaced squeezed vacuum state (DSVS), i.e. $|\alpha, \xi\rangle = D(\alpha)S(\xi)|0\rangle$ with $n_{\text{th}} = 0$. In this scenario, the average photon number is given by $\bar{n} = |\alpha|^2 + \sinh^2 r$ and we define β as the ratio of quantum squeezing and coherence, i.e., $\beta \equiv \sinh^2 r / |\alpha|^2$.

Now, we explore to what extent quantum squeezing can ensure the realization of the double-HS precision. From the Eq. (12), we obtain the photon-number fluctuation

$$\begin{aligned} \text{Var}(a^\dagger a) &= \frac{1}{2} \sinh^2 2r + |\alpha|^2 [\cosh 2r - \sinh 2r \cos(2\zeta - \vartheta)] \\ &= \frac{1}{2} \sinh^2 2r + \frac{\bar{n}}{1 + \beta} (\cosh 2r - \tau \sinh 2r), \end{aligned} \quad (25)$$

where $\tau \equiv \cos(2\zeta - \vartheta)$ reflects the phase configuration of

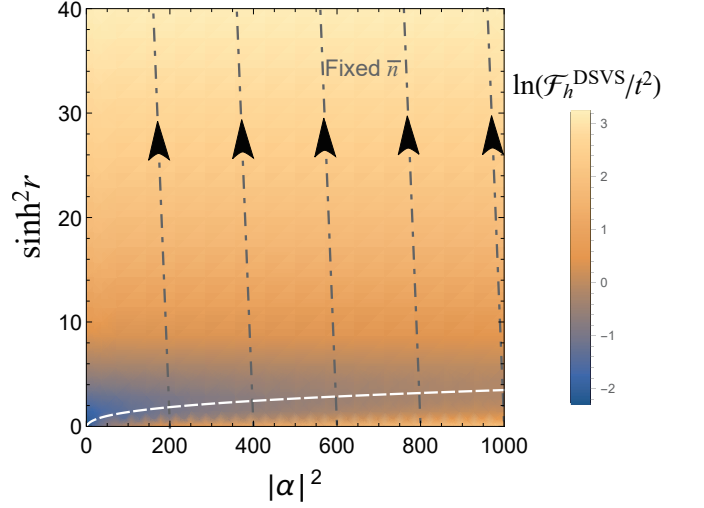


Figure 4. Density plot of the rescaled QFI $\ln(\mathcal{F}_h^{\text{DSVS}}/t^2)$ as a function of displacement $|\alpha|^2$ and squeezing $\sinh^2 r$ with the angle condition $\tau = 1$. The grey dot-dashed lines denote the states with a given average photon number (i.e., $\bar{n} = 200, 400, 600, 800, 1000$), and the arrow direction shows an increase with squeezing. The white dashed line shows the minimum of the rescaled QFI versus displacement and squeezing. Other parameters are the same as those in Fig. 3.

the initial optical state. Given the fact that $2\sinh^2 r \leq \sinh 2r < 2\sinh^2 r + 1$, it follows that

$$\begin{aligned} \text{Var}(a^\dagger a) &> \text{Var}_+ \\ &\equiv \frac{\bar{n}}{1 + \beta} \left[\frac{2\beta\bar{n}}{1 + \beta} (\beta + 1 - \tau) + 1 - \tau \right] \end{aligned} \quad (26)$$

for $\tau \geq 0$, and

$$\begin{aligned} \text{Var}(a^\dagger a) &\geq \text{Var}_- \\ &\equiv \frac{\bar{n}}{1 + \beta} \left[\frac{2\beta\bar{n}}{1 + \beta} (\beta + 1 - \tau) + 1 \right] \end{aligned} \quad (27)$$

for $\tau < 0$. When $\beta \gg 1/(2\bar{n})$, Eqs. (26) and (27) further suggest the scaling of quantum fluctuation

$$\text{Var}(a^\dagger a) \gtrsim \frac{\bar{n}}{1 + \beta} \left(\frac{2\beta^2\bar{n}}{1 + \beta} + 1 \right) \gtrsim \frac{2\beta^2}{(1 + \beta)^2} \bar{n}^2. \quad (28)$$

Based on the above analysis, we have $\text{Var}(a^\dagger a) \approx 2\bar{n}^2$, $\langle \mu | J_z^2 | \mu \rangle = N^2/4$, and $\text{Var}(J_z) = 0$ for a spin-coherent state with a large enough β and the angle $\theta = 0$. Consequently, the QFI (11) gives

$$\mathcal{F}_h^{\text{DSVS}} = \frac{4g^4}{\Delta^4} t^2 N^2 \text{Var}(a^\dagger a) \gtrsim \frac{8g^4}{\Delta^4} \frac{\beta^2}{(1 + \beta)^2} t^2 N^2 \bar{n}^2, \quad (29)$$

showing a novel existence of the double-HS. It is noticed that we also require the average photon and atom numbers satisfying $\Delta \gg g\sqrt{N} \gg g\sqrt{N^2/\bar{n}}$ (corresponding to the requirement in the time-averaged method) and the

squeezing satisfying $\beta \gg 1/(2\bar{n})$. We observe that the growth of squeezing can enhance measurement precision for a fixed number of atoms.

We now further ascertain the conditions under which the QFI increases with the quantum squeezing. In Fig. 4, the density plot depicts the rescaled QFI $\ln(\mathcal{F}_h^{\text{DSVS}}/t^2)$, as a function of displacement $|\alpha|^2$ and squeezing $\sinh^2 r$, with a fixed $\tau = 1$. For a given average photon number \bar{n} (indicated by the grey dot-dashed lines), the QFI first decreases and subsequently increases as the squeezing component rises. The white dashed line delineates the minimum of the QFI. We observe that, at least for the $\tau = 1$ case, squeezing is not always beneficial to the QFI for a small value of squeezing.

In Fig. 5a, the QFI $\mathcal{F}_h^{\text{DSVS}}$ depicts the role of squeezing parameter in terms of $\sinh^2 r$ and the phase parameter $\tau = \cos(2\zeta - \vartheta)$ for a fixed average photon number $\bar{n} = 1000$. The parameter space can be divided into two distinct regions: the QFI exhibits a monotonic increase with growing squeezing in region-I, while the QFI experiences a monotonic decrease as squeezing increases in region-II. Therefore, for $\tau < 0$, regardless of the squeezing value, an increase in the squeezing always leads to a growth of the QFI. Meanwhile, for $\tau < 0$, the phase parameter provides an additional positive effect to the QFI $\mathcal{F}_h^{\text{DSVS}} = 4g^4 t^2 N^2 \text{Var}(a^\dagger a) / \Delta^4$, see Fig. 5b. We thus can optimize the efficiency of the quantum resource (squeezing) to maximize the measurement precision by controlling the phase parameter ($\tau = -1$) in the presence of an imperfect squeezing light. Therefore, for a DSVS, the double-HS precision is attainable if the ratio β between the quantum squeezing and coherence is large enough $\beta \gg 1/(2\bar{n})$.

B. Optical coherent state with a spin-squeezed state

We have demonstrated the realization of a double-HS precision by building on optical squeezing. Now we further explore the role of spin squeezing in the metrological sensibility of measuring the magnetic field. To this end, we consider an initial state $|\psi\rangle = |\alpha\rangle \otimes |\phi\rangle$, comprising a classical coherent state $|\alpha\rangle$ for the optical component and a nonclassical spin-squeezed state [67–70] for the atomic component

$$|\phi\rangle = e^{-i\frac{\chi}{2}J_x^2} |1\rangle. \quad (30)$$

Here, $|1\rangle = |j, -j\rangle$ is the collective ground state with the eigenvalue $-N/2$, $\chi = 2\kappa t$ is the one-axis twisting angle and κ is the coupling constant. Then we have the fluctuation

$$\text{Var}(J_z) = \frac{1}{8}N \left[(N-1) \cos^{N-2} \chi - 2N \cos^{2N-2} \left(\frac{\chi}{2} \right) + N + 1 \right]. \quad (31)$$

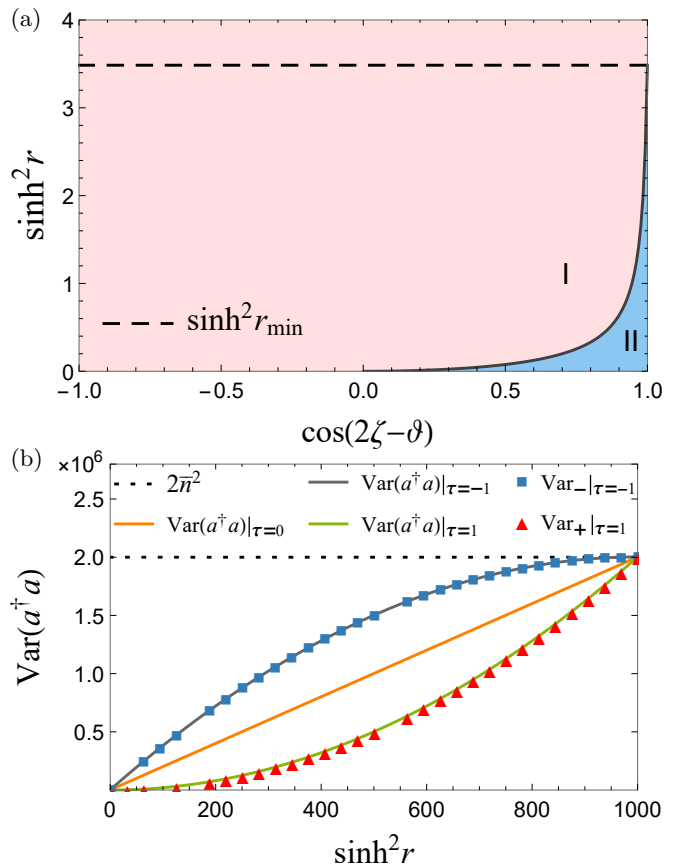


Figure 5. Monotonicity of the QFI $\mathcal{F}_h^{\text{DSVS}}$ and the photon-number fluctuation $\text{Var}(a^\dagger a)$ for DSVSs. (a) Monotonic regions of the QFI $\mathcal{F}_h^{\text{DSVS}}$ versus the squeezing $\sinh^2 r$ and the angle condition $\tau = \cos(2\zeta - \vartheta)$ with a given average photon number $\bar{n} = 1000$. The black line indicates the derivative zeros $\partial_{\sinh^2 r} \mathcal{F}_h^{\text{DSVS}} = 0$, dividing the parameter space into two regions: monotonically increasing region-I (pink) and monotonically decreasing region-II (cyan). The black dashed line $\sinh^2 r_{\min}$ denotes the squeezing value at the boundary when $\tau = 1$. (b) The photon-number fluctuation $\text{Var}(a^\dagger a)$ as a function of the squeezing $\sinh^2 r$ with a fixed average photon number $\bar{n} = 1000$ and specific angle conditions $\tau = 0, \pm 1$, respectively. The fluctuations for $\tau = -1$ (gray line), $\tau = 0$ (orange line), $\tau = 1$ (green line), their approximations $\text{Var}_-|_{\tau=-1}$ (blue squares) and $\text{Var}_+|_{\tau=1}$ (red triangles), and the maximum fluctuation $2\bar{n}^2$ (black dots), confirm the scalings Eqs. (26) and (27). Other parameters are the same as those in Fig. 3.

For the one-axis twisting angle $\chi = \pi + 2k\pi$ (k is integer), we have

$$\text{Var}(J_z) = \begin{cases} \frac{N^2}{4}, & \text{even } N; \\ \frac{N}{4}, & \text{odd } N. \end{cases} \quad (32)$$

Moreover, for $\chi = \pi/2 + k\pi$ and the spin number $N \gg 1$, we find $\text{Var}(J_z) \approx N^2/8$ is insusceptible to the parity of spin N . Here, we may choose the case $\chi = \pi + 2k\pi$ with an even N and $\text{Var}(a^\dagger a) = |\alpha|^2 = \bar{n} \gg \Delta^2/(2g^2)$ so

that the maximum QFI is given by

$$\begin{aligned} \mathcal{F}_h &= 4t^2 \left[\left(1 - \frac{2g^2}{\Delta^2} \bar{n} \right)^2 \text{Var}(J_z) + \frac{4g^4}{\Delta^4} \text{Var}(a^\dagger a) \langle J_z^2 \rangle \right] \\ &\gtrsim \frac{4g^4}{\Delta^4} t^2 N^2 \bar{n}^2. \end{aligned} \quad (33)$$

By comparison, we observe that both Eq. (23) and Eq. (33) give a double-HS precision. In the latter, the utilization of atom-number fluctuation results in $\mathcal{F}_h \propto \bar{n}^2 \text{Var}(J_z)$. Similarly, we could also obtain the maximum QFI $\mathcal{F}_h \approx 12g^4 t^2 N^2 \bar{n}^2 / \Delta^2$ in frequency estimation by inducing both the light and spin squeezing with $\chi = \pi + 2k\pi$, $|\alpha| = n_{\text{th}} = 0$ and large even N .

V. CONCLUSION AND DISCUSSION

In a prototypical and theoretically significant cavity QED, TC model, we have explored the feasibility of achieving double-HS precision. The derived effective Hamiltonian (6) unveils the emergence of the coherent averaging mechanism even in estimating a non-global parameter, which leads to the HS precision for the photon number when classical states serve as the probing entities. The underlying cause of the HL scaling resides in the fact that the evolved atom state (i.e., quantum bus) captures the accumulated phase arising from the interaction between the cavity field and the quantum bus. Hence, measuring the quantum bus suffices to achieve this HS precision even without nonclassical inputs.

Considering nonclassical inputs, we have derived an analytical expression for the QFI, showing that the double-HS precision is attainable through the introduction of either the photon-number fluctuation via optical squeezing or the atom-number fluctuation via spin squeezing. In addition, we have also investigated differ-

ent metrological scenarios, where optical squeezing and coherence coexist. In such instances, we have observed that an increase in the squeezing can decrease measurement precision when the photon number remains fixed and squeezing is small. Judiciously adjusting the phase parameter could offer a viable solution to mitigate the imperfect squeezing.

Our work goes beyond the conventional coherent averaging mechanism, extending the quantum bus from a single atom to N atoms and from estimating a global parameter to a non-global one. These extensions provide deeper insights into the realization of the double-HS precision in the models with star-like long-range interactions. Our findings hold immediate implications for determining the minimum quantum resource prerequisites for high-precision metrology in more intricate metrological networks featuring multiple quantum buses. Recent remarkable experimental advancements in attaining strong coupling [56–59, 71–73], as well as the development of the TC model [74], also instill optimism regarding the prospective realization of our theoretical framework.

ACKNOWLEDGMENTS

This work is supported by the National Natural Science Foundation of China Key grants No. 92365202, No. 12134015, No. 12121004, and the National Key Research and Development Program of China No. 2022YFA1404102. Y.G.S. is supported by the National Natural Science Foundation of China grant No. 12247158, the ‘‘Wuhan Talent’’ (Outstanding Young Talents), and the Postdoctoral Innovative Research Post in Hubei Province. HLS was supported by the European Commission through the H2020 QuantERA ERA-NET Cofund in Quantum Technologies project ‘‘MENTA’’ and the Hefei National Laboratory.

-
- [1] J. J. Bollinger, W. M. Itano, D. J. Wineland, and D. J. Heinzen, *Phys. Rev. A* **54**, R4649 (1996).
 - [2] L. Pezzè, A. Smerzi, M. K. Oberthaler, R. Schmied, and P. Treutlein, *Rev. Mod. Phys.* **90**, 035005 (2018).
 - [3] V. Giovannetti, S. Lloyd, and L. Maccone, *Phys. Rev. Lett.* **96**, 010401 (2006).
 - [4] P. Hyllus, W. Laskowski, R. Krischek, C. Schwemmer, W. Wieczorek, H. Weinfurter, L. Pezzè, and A. Smerzi, *Phys. Rev. A* **85**, 022321 (2012).
 - [5] G. Tóth, *Phys. Rev. A* **85**, 022322 (2012).
 - [6] N. Li and S. Luo, *Phys. Rev. A* **88**, 014301 (2013).
 - [7] Z. Ren, W. Li, A. Smerzi, and M. Gessner, *Phys. Rev. Lett.* **126**, 080502 (2021).
 - [8] T. Monz, P. Schindler, J. T. Barreiro, M. Chwalla, D. Nigg, W. A. Coish, M. Harlander, W. Hänsel, M. Hennrich, and R. Blatt, *Phys. Rev. Lett.* **106**, 130506 (2011).
 - [9] C. M. Caves, *Phys. Rev. D* **23**, 1693 (1981).
 - [10] C. M. Caves, K. S. Thorne, R. W. P. Drever, V. D. Sandberg, and M. Zimmermann, *Rev. Mod. Phys.* **52**, 341 (1980).
 - [11] D. F. Walls, *Nature* **306**, 141 (1983).
 - [12] V. V. Dodonov, *J. Opt. B: Quantum Semiclassical Opt.* **4**, R1 (2002).
 - [13] H. Vahlbruch, S. Chelkowski, B. Hage, A. Franzen, K. Danzmann, and R. Schnabel, *Phys. Rev. Lett.* **97**, 011101 (2006).
 - [14] H. Vahlbruch, S. Chelkowski, B. Hage, A. Franzen, K. Danzmann, and R. Schnabel, *Phys. Rev. Lett.* **95**, 211102 (2005).
 - [15] K. McKenzie, D. A. Shaddock, D. E. McClelland, B. C. Buchler, and P. K. Lam, *Phys. Rev. Lett.* **88**, 231102 (2002).
 - [16] K. McKenzie, N. Grosse, W. P. Bowen, S. E. Whitcomb, M. B. Gray, D. E. McClelland, and P. K. Lam, *Phys. Rev. Lett.* **93**, 161105 (2004).

- [17] W. Muessel, H. Strobel, D. Linnemann, T. Zibold, B. Juliá-Díaz, and M. K. Oberthaler, *Phys. Rev. A* **92**, 023603 (2015).
- [18] A. D. Ludlow, M. M. Boyd, J. Ye, E. Peik, and P. O. Schmidt, *Rev. Mod. Phys.* **87**, 637 (2015).
- [19] A. Louchet-Chauvet, J. Appel, J. J. Renema, D. Oblak, N. Kjaergaard, and E. S. Polzik, *New J. Phys.* **12**, 065032 (2010).
- [20] E. M. Kessler, P. Kómár, M. Bishof, L. Jiang, A. S. Sørensen, J. Ye, and M. D. Lukin, *Phys. Rev. Lett.* **112**, 190403 (2014).
- [21] B. P. Abbott *et al.*, *Rep. Prog. Phys.* **72**, 076901 (2009).
- [22] D. Budker and M. Romalis, *Nat. Phys.* **3**, 227 (2007).
- [23] R. J. Sewell, M. Koschorreck, M. Napolitano, B. Dubost, N. Behbood, and M. W. Mitchell, *Phys. Rev. Lett.* **109**, 253605 (2012).
- [24] F. Troiani and M. G. A. Paris, *Phys. Rev. Lett.* **120**, 260503 (2018).
- [25] Y. Chu, S. Zhang, B. Yu, and J. Cai, *Phys. Rev. Lett.* **126**, 010502 (2021).
- [26] Y. Su, W. Lu, and H.-L. Shi, (2023), arXiv:2307.16166 [quant-ph].
- [27] J. B. Brask, R. Chaves, and J. Kołodyński, *Phys. Rev. X* **5**, 031010 (2015).
- [28] M. Genovese, *J. Opt.* **18**, 073002 (2016).
- [29] S. Z. Ang, R. Nair, and M. Tsang, *Phys. Rev. A* **95**, 063847 (2017).
- [30] J. Řehaček, Z. Hradil, B. Stoklasa, M. Paúr, J. Grover, A. Krzic, and L. L. Sánchez-Soto, *Phys. Rev. A* **96**, 062107 (2017).
- [31] X. Deng, S. Li, Z.-J. Chen, Z. Ni, Y. Cai, J. Mai, L. Zhang, P. Zheng, H. Yu, C.-L. Zou, S. Liu, F. Yan, Y. Xu, and D. Yu, (2023), arXiv:2306.16919 [quant-ph].
- [32] X.-J. Tan, L. Qi, L. Chen, A. J. Danner, P. Kanchanawong, and M. Tsang, *Optica* **10**, 1189 (2023).
- [33] S. L. Braunstein and C. M. Caves, *Phys. Rev. Lett.* **72**, 3439 (1994).
- [34] Y. Chu, X. Li, and J. Cai, *Phys. Rev. Lett.* **130**, 170801 (2023).
- [35] H.-L. Shi, X.-W. Guan, and J. Yang, (2023), arXiv:2308.03696 [quant-ph].
- [36] Q.-K. Wan, H.-L. Shi, and X.-W. Guan, (2023), arXiv:2305.08045 [quant-ph].
- [37] L. Campos Venuti and P. Zanardi, *Phys. Rev. Lett.* **99**, 095701 (2007).
- [38] T. Ilias, D. Yang, S. F. Huelga, and M. B. Plenio, *PRX Quantum* **3**, 010354 (2022).
- [39] V. Montenegro, U. Mishra, and A. Bayat, *Phys. Rev. Lett.* **126**, 200501 (2021).
- [40] I. Frérot and T. Roscilde, *Phys. Rev. Lett.* **121**, 020402 (2018).
- [41] P. Zanardi, M. G. A. Paris, and L. Campos Venuti, *Phys. Rev. A* **78**, 042105 (2008).
- [42] L. Garbe, M. Bina, A. Keller, M. G. A. Paris, and S. Felicetti, *Phys. Rev. Lett.* **124**, 120504 (2020).
- [43] L. J. Fiderer and D. Braun, *Nat Commun* **9**, 1351 (2018).
- [44] W. Liu, M. Zhuang, B. Zhu, J. Huang, and C. Lee, *Phys. Rev. A* **103**, 023309 (2021).
- [45] Z. Li, S. Colombo, C. Shu, G. Velez, S. Pilatowsky-Cameo, R. Schmied, S. Choi, M. Lukin, E. Pedrozo-Peñañiel, and V. Vuletić, *Science* **380**, 1381 (2023).
- [46] X. Long, W.-T. He, N.-N. Zhang, K. Tang, Z. Lin, H. Liu, X. Nie, G. Feng, J. Li, T. Xin, Q. Ai, and D. Lu, *Phys. Rev. Lett.* **129**, 070502 (2022).
- [47] S. Pang and A. N. Jordan, *Nat. Commun.* **8**, 14695 (2017).
- [48] J. Yang, S. Pang, and A. N. Jordan, *Phys. Rev. A* **96**, 020301 (2017).
- [49] J. Yang, S. Pang, Z. Chen, A. N. Jordan, and A. del Campo, *Phys. Rev. Lett.* **128**, 160505 (2022).
- [50] D. Braun and J. Martin, *Nat. Commun.* **2**, 223 (2011).
- [51] J. M. E. Fraïsse and D. Braun, *Ann. Phys.* **527**, 701 (2015).
- [52] D. Braun, G. Adesso, F. Benatti, R. Floreanini, U. Marzolino, M. W. Mitchell, and S. Pirandola, *Rev. Mod. Phys.* **90**, 035006 (2018).
- [53] M. Tavis and F. W. Cummings, *Phys. Rev.* **170**, 379 (1968).
- [54] D. F. James and J. Jerke, *Can. J. Phys.* **85**, 625 (2007).
- [55] B. W. Shore and P. L. Knight, *J. Mod. Opt.* **40**, 1195 (1993).
- [56] D. I. Schuster, A. A. Houck, J. A. Schreier, A. Wallraff, J. M. Gambetta, A. Blais, L. Frunzio, J. Majer, B. Johnson, M. H. Devoret, S. M. Girvin, and R. J. Schoelkopf, *Nature* **445**, 515 (2007).
- [57] F. Brennecke, R. Mottl, K. Baumann, R. Landig, T. Donner, and T. Esslinger, *Proc. Natl. Acad. Sci. U.S.A.* **110**, 11763 (2013).
- [58] S. M. Spillane, T. J. Kippenberg, K. J. Vahala, K. W. Goh, E. Wilcut, and H. J. Kimble, *Phys. Rev. A* **71**, 013817 (2005).
- [59] J. R. Buck and H. J. Kimble, *Phys. Rev. A* **67**, 033806 (2003).
- [60] X.-B. Wang, T. Hiroshima, A. Tomita, and M. Hayashi, *Phys. Rep.* **448**, 1 (2007).
- [61] C. Weedbrook, S. Pirandola, R. García-Patrón, N. J. Cerf, T. C. Ralph, J. H. Shapiro, and S. Lloyd, *Rev. Mod. Phys.* **84**, 621 (2012).
- [62] J. Liu, H. Yuan, X.-M. Lu, and X. Wang, *J. Phys. A: Math. Theor.* **53**, 023001 (2019).
- [63] Yuguo Su and X. Wang, *Results Phys.* **24**, 104159 (2021).
- [64] J. M. Radcliffe, *J. Phys. A: Gen. Phys.* **4**, 313 (1971).
- [65] H. F. Baker, *Proc. Lond. Math. Soc.* **s1-34**, 347 (1901).
- [66] J. Johansson, P. Nation, and F. Nori, *Comput. Phys. Commun.* **183**, 1760 (2012).
- [67] M. Kitagawa and M. Ueda, *Phys. Rev. A* **47**, 5138 (1993).
- [68] J. Ma, X. Wang, C. Sun, and F. Nori, *Phys. Rep.* **509**, 89 (2011).
- [69] X. Wang, A. Miranowicz, Y.-x. Liu, C. P. Sun, and F. Nori, *Phys. Rev. A* **81**, 022106 (2010).
- [70] Y. Su, H. Liang, and X. Wang, *Phys. Rev. A* **102**, 052423 (2020).
- [71] J. M. Fink, M. Goeppl, M. Baur, R. Bianchetti, P. J. Leek, A. Blais, and A. Wallraff, *Nature* **454**, 315 (2008).
- [72] T. Allcock, W. Langbein, and E. A. Muljarov, *Phys. Rev. Lett.* **128**, 123602 (2022).
- [73] Y. Liu, Z. Wang, P. Yang, Q. Wang, Q. Fan, S. Guan, G. Li, P. Zhang, and T. Zhang, *Phys. Rev. Lett.* **130**, 173601 (2023).
- [74] J. M. Fink, R. Bianchetti, M. Baur, M. Göppl, L. Steffen, S. Filipp, P. J. Leek, A. Blais, and A. Wallraff, *Phys. Rev. Lett.* **103**, 083601 (2009).